



Published in final edited form as:

Invest Ophthalmol Vis Sci. 2010 January ; 51(1): 264–271. doi:10.1167/iovs.08-2014.

Clinical Evaluation of the Proper Orthogonal Decomposition Framework for Detecting Glaucomatous Changes in Human Subjects

Madhusudhanan Balasubramanian¹, Christopher Bowd¹, Robert N. Weinreb¹, Gianmarco Vizzeri¹, Luciana M. Alencar¹, Pamela A. Sample¹, Neil O'Leary², and Linda M. Zangwill¹

¹Hamilton Glaucoma Center, Department of Ophthalmology, University of California, San Diego, La Jolla, California

²Department of Optometry and Visual Science, City University, London, United Kingdom

Abstract

Purpose—To evaluate the new proper orthogonal decomposition (POD) framework for detecting glaucomatous progression from HRT topographies of human subjects and compare it with HRT topographic change analysis (TCA).

Methods—Of 267 eyes of 187 participants with ≥ 4 retinal tomographic examinations in the University of California, San Diego Diagnostic Innovations in Glaucoma Study (DIGS), 21 eyes were of longitudinally *normal subjects* and 36 eyes progressed by stereophotographs or visual field–guided progression analysis (*progressors*). All others were considered nonprogressing (*nonprogressors*; $n = 210$ eyes). POD parameters of Euclidean distance (L_2 norm), image Euclidean distance, and correlation were computed, and their area under receiver operating characteristic curves (AUC) in differentiating progressors from nonprogressors and normal subjects were compared to the TCA parameters of the number of superpixels with significant decrease in retinal height (*red pixels*), size of the largest cluster of red pixels (*CSIZE*), and *CSIZE%* of disc size, all within the optic disc margin.

Results—AUCs of the best performing POD L_2 norm and TCA red pixel parameters in differentiating progressors from normal subjects were both 0.86 and in differentiating progressors from nonprogressors were 0.68 and 0.64, respectively; the AUC differences were not statistically significant.

Conclusions—The POD framework, which can detect and confirm glaucomatous changes in a single follow-up visit, provides a performance similar to that of TCA in differentiating progressors from normal subjects and nonprogressors.

Because of the chronic and progressive nature of glaucoma, detection of progressive structural changes in the optic nerve head (ONH) region and progressive visual function changes is an important component of clinical management of the disease. Detecting progressive changes may be challenging because of any inherent variability in the appearance of the ONH due to ocular (for example, due to fluctuations in intraocular pressure) or systemic conditions (for example, due to changes in blood pressure), variability in the structural and functional

Corresponding author: Linda M. Zangwill, Hamilton Glaucoma Center, Department of Ophthalmology, University of California, San Diego, 9500 Gilman Drive 0946, La Jolla, CA 92093; zangwill@glaucoma.ucsd.edu.

Disclosure: **M. Balasubramanian**, Heidelberg Engineering (F); **C. Bowd**, Pfizer (F), Lacle Electronics (F); **R.N. Weinreb**, Heidelberg Engineering (F), Carl Zeiss Meditec (F, C); **G. Vizzeri**, None; **L.M. Alencar**, None; **P.A. Sample**, Carl Zeiss Meditec (F), Haag-Streit (F), Welch-Allyn (F); **N. O'Leary**, None; **L.M. Zangwill**, Heidelberg Engineering (F), Carl Zeiss Meditec (F), Optovue (F)

measurements due to the instruments used in the examinations, and the slowly progressing nature of the disease.

The Heidelberg Retina Tomograph (HRT; Heidelberg Engineering, GmbH, Heidelberg, Germany) is a confocal scanning laser ophthalmoscope (CSLO) commonly used in ophthalmology clinics for monitoring glaucomatous structural changes in the ONH region. The HRT captures the three-dimensional architecture of an ONH by acquiring high-resolution optical section images of the ONH at various depths with less dependence on pupil dilation compared with stereophotography and therefore allows a routine and rapid clinical analysis of the ONH for detecting progressive structural changes. HRT software constructs a three-dimensional profile of ONH topography from the optical section images. Localized pixel-level ONH changes can be detected from the ONH topographies by using statistical change detection algorithms.^{1,2}

The new proper orthogonal decomposition (POD) framework was recently introduced for detecting structural glaucomatous changes in the ONH, and the diagnostic performance of the POD framework has been demonstrated in ONH examinations of primate eyes under experimental glaucomatous conditions.³ In this work, we evaluated the clinical diagnostic performance of the POD framework for detecting glaucomatous progression in human subjects and compared it with the HRT topographic change analysis (TCA).

Methods

Subjects

All eligible participants from the University of California, San Diego (UCSD) Diagnostic Innovations in Glaucoma Study (DIGS) with at least four good-quality retinal tomographic examinations (HRT-II; Heidelberg Engineering), at least five good-quality Standard Automated Perimetry (SAP; Humphrey HFAII, Carl Zeiss Meditec, Dublin, CA) visual field examinations (SITA standard and full-threshold examinations), and at least two good-quality stereophotographs (TRC-SS; Topcon Instruments Corp. of America, Paramus, NJ) of the optic disc were included in the study (267 eyes of 187 participants). HRT-II examinations with a mean pixel height standard deviation (MPHSD) $<50 \mu\text{m}$, even image exposure, and good centering were considered to be of good quality; SAP visual field examinations with fewer than 25% false positives, false negatives and fixation losses and no observable testing artifacts were considered to be reliable; stereophotographs that were assessed to be of fair to excellent quality by trained graders were considered to be acceptable.

Two hundred forty-six eyes of 167 patients were categorized as progressed and nonprogressed (details presented later) based on visual function changes by SAP-guided progression analysis (GPA; Humphrey Field Analyzer, software ver. 4.2) and optic disc progression grading by stereophotography. For each eye, the baseline visual field examinations for SAP GPA and the baseline stereophotograph for optic disc progression grading were within 6 months of the HRT-II baseline examination date. Similarly, the last visual field examination for SAP GPA and the last stereophotograph for progression grading were within 6 months of the last HRT-II examination date.

An additional 21 eyes of 20 participants were longitudinally normal eyes (*normal subjects*) with no history of IOP $> 22 \text{ mm Hg}$, normal-appearing optic disc by stereophotography and SAP visual field examination results within normal limits (median age, 62.7 years; median HRT-II follow-up, 0.5 year).

Glaucomatous progression in the 246 patient eyes was defined based on likely progression by SAP GPA or progression by stereophotographs of the optic disc. Progressive changes in the

stereophotographic appearance of the optic disc between the baseline and the last stereophotograph of an eye (patient name, diagnosis, and temporal order of stereophotographs were masked) were assessed by two observers based on a decrease in the neuroretinal rim thickness, appearance of a new retinal nerve fiber layer (RNFL) defect, or increase in the size of a preexisting RNFL defect. Any differences in assessment between these two observers were adjudicated by a third observer. Thirty-six eyes of 33 participants progressed by stereophotographs and/or showed likely progression in SAP GPA (*progressors*) and the rest of the 210 eyes of 148 participants were considered nonprogressing (*nonprogressors*). Table 1 provides a detailed summary of the progressors and nonprogressors. The UCSD Institutional Review Board approved the study methodologies and all protocols adhered to the Declaration of Helsinki guidelines for research in human subjects and the Health Insurance Portability and Accountability Act (HIPAA).

HRT Image Processing

TCA change probabilities were computed for all study participants (HRT 3 software; HRTS Glaucoma Module, ver. 3.1.2.5; Heidelberg Engineering). For quantitative analysis, TCA superpixel change probabilities of each follow-up examination and all topographies aligned with the baseline topography of each eye were exported from the software. (TCA change probability exports are available as .txt files, and the topographies are available as .raw files; all analyses by MATLAB ver. 7.4.0; The Mathworks, Inc., Natick, MA.)

Using the change probabilities and the superpixel mean difference images exported from the software, a change significance map was constructed for each follow-up examination by identifying the superpixel locations with significant decrease in retinal height from the baseline examination (i.e., the locations with negative height change in the mean difference image and change probability <0.05). As in the software (HRTS glaucoma module, ver. 3.1.2.5), any significantly changed superpixel locations with fewer than four significantly changed superpixel neighbors were discarded. After any isolated locations were filtered from the change significance maps, clinically significant TCA change locations were detected by identifying the superpixel locations with changes repeatable in two of two, three of three, or three of four most recent follow-up examinations, depending on the number of follow-up examinations available at the time of evaluation (personal communication, Heidelberg Engineering, 2007). The spatially filtered and clinically significant change significance maps were used to compute 3 TCA change summary parameters: (1) total number of superpixel locations with a significant decrease in retinal height within the optic disc margin (*red pixels*), (2) size of the largest cluster of red pixels within the optic disc margin (*CSIZE*), and (3) proportion of CSIZE to disc size in percent (*CSIZE%*).

The POD Framework

The details of the POD framework have been published.³ In brief, for detecting structural progression in an eye from a baseline condition, the POD mathematical technique constructs a subspace of baseline ONH topographies, called a *baseline subspace*, from a set of ONH topographies of the eye at baseline. A baseline subspace contains all possible topographies of an eye at baseline derived from the measurement variability observed at baseline. Therefore, a baseline subspace uniquely represents the structural appearance of an eye at baseline by incorporating topographic measurement variability and any inherent structural variability observed in the baseline examinations. In follow-up examination evaluations, follow-up topographies are compared with the topographies in the baseline subspace that appear structurally more similar and also geometrically closer (in a least-squares error sense) to the respective follow-up topographies. Choosing baseline topographies from the baseline subspace that appear more similar to the follow-up topographies for detecting progression is expected to reduce false positives and improve the specificity of detecting glaucomatous changes.

At present, the POD framework does not have a graphic representation of locations of change as in the HRT TCA. The POD framework uses several change summary parameters (described later) to quantify change in a follow-up examination from baseline: A minimum bounding rectangular region covering a manually drawn optic disc contour line is constructed in each of the topographies to select topographic measurements within the optic disc region. These regions are marked by dotted rectangles in Figures 3a, 3b, 4a, and 4b. Glaucomatous changes are summarized by comparing topographic measurements from locations with decreases in retinal height from baseline within the optic disc margin in the follow-up examinations and their respective baseline subspace representations. The changes were quantified using the summary parameters of (1) Euclidean distance (L_2 norm), (2) image Euclidean distance (IMED), and (3) correlation. L_2 norm and IMED parameters measure the degree of dissimilarity between a follow-up topography and its baseline subspace representation; therefore, higher values indicate more changes in the follow-up from the baseline; correlation measures the degree of similarity between a follow-up topography and its baseline subspace representation, therefore, lower values indicate more changes in the follow-up examination from the baseline.

Performance Analysis

The POD and TCA summary parameters of the last HRT examination of an eye were used to detect glaucomatous progression (however, TCA summary parameters of the last HRT examination were based on changes repeatable in the three latest HRT follow-up examinations as per the HRT-3 software requirements). For evaluating the diagnostic performance of the POD framework compared to TCA, the last HRT follow-up examinations of the progressors were considered as progressing and of the normal subjects and nonprogressors were considered stable. The diagnostic performance of the POD and TCA summary parameters in differentiating progressing eyes from stable eyes were measured by determining the area under their receiver operating characteristic curves (AUC). The performance of the POD summary parameters of L_2 norm, IMED, and correlation was compared with the TCA summary parameters of total number of red pixels, CSIZE, and CSIZE%.

Results

Table 2 lists a performance summary of the POD and TCA parameters for detecting glaucomatous progression in the set of 36 progressors, 21 normal subjects, and 210 nonprogressors. In differentiating progressors from normal subjects, the L_2 norm parameter resulted in the largest AUC (0.86) among the POD parameters, and all the TCA parameters resulted in the same AUC of 0.86. Figure 1 shows the corresponding ROC curves of the POD L_2 norm and the TCA red pixels parameters.

In differentiating progressors from nonprogressors, L_2 norm resulted in the largest AUC (0.68) among the POD parameters and red pixels resulted in the largest AUC (0.64) among the TCA parameters. The difference in the AUC of 0.04 (95% confidence interval [CI], -0.08 to 0.14) did not reach statistical significance ($P = 0.28$). Figure 2 shows the corresponding ROC curves of the POD L_2 norm and the TCA red pixels parameters.

Figure 3 shows an example of a normal subject and Figure 4 shows an example of a progressor with progressive glaucomatous changes by stereophotography and likely progression by SAP GPA. Changes in a follow-up examination can be observed visually by comparing the follow-up examinations with their respective baseline subspace representations; quantitatively, large POD L_2 summary parameters indicate evidence of change from baseline. In Figure 3, there was no evidence of changes in the follow-up topographies from the baseline condition. The lack of change can be observed by the obvious similarity of each of the follow-up topographies shown in Figure 3a with their respective baseline subspace representations shown immediately below them in Figure 3b.

In contrast, changes can be observed in the follow-up topographies of the example progressor shown in Figure 4a by comparing them with their respective baseline subspace representations shown immediately below them in Figure 4b. Because retinal topographic measurements have a wider range, changes may not be visually obvious in the follow-up topographies shown in Figure 4; therefore, for demonstration, rim thickness changes in the inferior location of the example progressor for a follow-up examination in July 2007 (Jul07) are marked manually in Figure 4. For this example progressor, Figure 5a shows an enlarged mean topography from the last follow-up examination in Jul07 and its baseline subspace representation; Figure 5b shows the corresponding mean follow-up reflectance image and its baseline subspace representation; Figure 5c shows the baseline and last follow-up stereophotographs used for assessing glaucomatous changes by stereophotography; Figure 5d shows the SAP GPA of the earliest visual field follow-up examination with evidence of likely progression by GPA. Glaucomatous changes can be observed in the inferior optic disc location between the 5- and 8-o'clock positions in Figures 5a and 5b by comparing the follow-up topography/reflectance images with their respective baseline subspace representations. Structural glaucomatous changes of rim thinning and optic cup enlargement were visually more obvious in the HRT follow-up reflectance image in Figure 5b compared with the HRT follow-up topography in Figure 5a. GPA showed the corresponding visual field changes in the superior hemifield location. Overall differences between follow-up topographies and their POD baseline subspace representations also are summarized by large L_2 norm values of the progressor example in Figure 4b compared with the normal eye in Figure 3b (see also Fig. 6a for the trend plot of these POD L_2 norm parameter values).

Figures 3c and 4c show the TCA superpixel change significance maps for the normal and the progressor examples, indicating locations in the ONH regions with a significant decrease in retinal height from the baseline condition. Figure 6 shows the POD L_2 norm parameter trends and the TCA red pixels parameter trends of the normal (shown in Fig. 3) and the progressor (shown in Fig. 4) examples.

Discussion

In this work, we showed that the clinical diagnostic performance of the POD framework measured with AUC was similar to TCA in detecting glaucomatous changes from the HRT-II examinations of participants in the DIGS. AUCs of both the POD and TCA summary parameters were moderate in differentiating the progressors from normal subjects (AUC = 0.86) and low in differentiating the progressors from nonprogressors (AUC = 0.68 and 0.64, respectively), and the differences were not statistically significant. It should be noted that we used only the last HRT examinations of each of the study participants for calculating the diagnostic accuracies (AUC) of the POD framework and TCA. Therefore, the TCA parameters were derived from the three or four latest HRT examinations to provide high specificity in normal subjects and nonprogressors (i.e., changes repeatable in three of three or three of four most recent HRT follow-up examinations), whereas, the POD summary parameters were calculated only from the last HRT follow-up examination of a study participant and provide a similar diagnostic performance. For example, in the POD and TCA parameter trend of the example progressor shown in Figure 6, both the POD L_2 norm parameter and the TCA red pixels parameter detected change in the last follow-up. However, it can also be observed that the POD L_2 norm parameter detected change at the first follow-up examination (i.e., Sep02 examination in Fig. 6a) whereas, the TCA red pixels parameter detected change at the 4th follow-up (i.e., Nov06 examination in Fig. 6b). Quantitative analysis of determining the earliest glaucomatous changes in progressors, while maintaining high specificity in normal subjects and nonprogressors, is a topic of future study in which we will examine this strength of the POD framework.

Low diagnostic accuracies observed in both the POD framework and TCA when differentiating progressors from nonprogressors may be due to false classifications by the respective methods and/or any inaccuracies in the gold standard used to identify the nonprogressors based on the absence of progression by stereophotographs and SAP GPA. Therefore, some of the eyes in the nonprogressors group that were classified as progressors by the POD framework and TCA may correspond to eyes in early stages of progression that are not yet detected by stereophoto or visual field assessment. This possibility is in part supported by the fact that the diagnostic accuracies of both the techniques were high when differentiating progressors from normal subjects (AUCs = 0.86).⁴ Longer follow-up of these eyes is needed to determine the proportion of eyes in the nonprogressors group classified as progressors by the POD framework and TCA that later develop optic disc and/or visual field damage, which can be considered early detection and the proportion that remain stable which can be considered false positives.

At the core of the new POD framework is the construction of a unique baseline subspace in each eye that captures the topographic measurement variability and inherent structure variability at a baseline condition using the POD mathematical procedure. In contrast to the generalized subspaces often used in the conventional Fourier and wavelet transformations, the POD ensures that the baseline subspace constructed is optimal and, more important, unique to a given eye. Adaptive wavelet transforms constructed using the lifting scheme may be useful in generating an eye-specific baseline subspace similar to POD.⁵

There are several advantages of the POD framework. First, it can detect glaucomatous changes in a follow-up examination without requiring additional follow-up examinations to confirm the detected change, while maintaining high specificity. In contrast, TCA requires two or three follow-up confirmation examinations to achieve high specificity. The ability to detect change earlier in progressing eyes while maintaining high specificity in stable eyes without requiring several confirmations is particularly important in identifying glaucomatous progression for clinical decision-making and in randomized clinical trials.

Second, the POD framework allows the use of one or more HRT examinations to define a baseline condition and does not limit the number of scans or examinations that can be used to define a baseline or a follow-up condition. Because both the POD framework and TCA compare follow-up topographies to the baseline, estimates of topographic measurement variability at baseline is essential for differentiating glaucomatous changes from nonglaucomatous measurement variations (for e.g., due to measurement variability, or ONH structural variations due to fluctuations in intraocular pressure). Although acquiring more topographic scans per examination may improve the estimates of topographic measurement variability, it may not be logistically feasible in clinical practice; therefore, for this analysis we used three topographic scans per ONH examination that are automatically acquired with the HRT-II.⁶ However, acquiring one or more additional examinations within a short interval at the baseline condition can improve the variability estimates at baseline.⁷ The POD framework can easily use multiple baseline examinations to improve the estimates of baseline variability. For example, the POD L_2 norm parameter trend plots of an example progressor and a normal subject shown in Figure 7 indicate the inherent learning ability of the POD framework to incorporate two examinations within 6 months' duration, to define a baseline condition and improve the estimates of measurement variability at baseline (shaded region in the trend plots in Fig. 7). This feature of the POD framework can also be used to easily update the baseline subspace of an eye, which may improve the estimates of topographic measurement variability when the baseline condition changes—for example, after an IOP reduction surgery or after glaucoma medication. Statistical significance of the potential improvements in detecting change with multiple baseline examinations will be evaluated in a future work.

In the current analysis, the POD framework does not have a graphic representation of locations of change in the follow-up topography. However, one of the advantages of the POD framework is that other statistical and computational pixel-wise change detection algorithms can be integrated with the POD framework. For example, after constructing the baseline subspace representations of follow-up topographies, pixel-wise changes between follow-up topographies and their respective baseline subspace representations can be estimated using a statistical procedure as in the TCA method (i.e., the POD framework allows incorporation of the strengths of other progression analysis techniques). Inclusion of other pixel-wise change detection algorithms within the POD framework will be studied separately in a future work.

The POD framework for glaucomatous change detection requires the follow-up topographies to be aligned to the baseline topographies, as required by all pixel-wise change detection algorithms. In this work, the POD parameters were calculated from the topographies that were aligned using the standard alignment procedure available in the HRT 3 software. Theoretically, the IMED parameter can account for small misalignments between baseline and follow-up topographies compared with the L_2 norm parameter in the POD framework.^{3,8} However, the diagnostic accuracy of the IMED parameter is similar to the L_2 norm parameter indicating no significant misalignment among the topographies when using the alignment procedure available in the HRT-3 software.

One of the limitations of this study is the small number of progressors ($n = 36$ eyes) and normal subjects ($n = 21$ eyes) available for evaluating the diagnostic performance of the POD framework and TCA. A larger number of progressing eyes may improve the confidence interval of the AUC diagnostic measures. However, the study population size in the current analysis is comparable to other similar studies^{2,9,10} and, like other studies, is restricted by the slowly progressing nature of glaucoma.

For clinical use of the POD framework, parameter cutoffs that provide 95% detection specificity in control normal subjects and patients with stable glaucoma can be used to define glaucomatous progression by HRT topographies as in the TCA parameters.⁴ POD parameter cutoffs can be estimated as the 95th percentile values of these parameters in control normal subjects and patients with stable glaucoma and will be studied in a future work.

In summary, the POD framework shows promise for detecting glaucomatous progression in human subjects and provides an overall performance similar to that of HRT TCA. Unique advantages of the POD framework include its ability to detect and confirm changes by using a single follow-up examination, while maintaining high specificity; its inherent learning capability of using multiple baseline examinations, when available, to improve the estimates of topographic measurement variability; and the ability to easily update the progression analysis when the baseline condition in an eye changes. Further study is necessary to determine whether the unique strengths of the POD framework can significantly improve the diagnostic accuracy of the method.

Acknowledgments

Supported in part by Heidelberg Engineering, GmbH; National Eye Institute Grants EY08208 (PAS) and EY11008 (LMZ); and participant incentive grants in the form of glaucoma medication at no cost from Alcon Laboratories Inc., Allergan, Pfizer Inc., and SANTEN Inc. (PAS).

References

1. Chauhan BC, Blanchard JW, Hamilton DC, LeBlanc RP. Technique for detecting serial topographic changes in the optic disc and peripapillary retina using scanning laser tomography. *Invest Ophthalmol Vis Sci* 2000;41(3):775–782. [PubMed: 10711693]

2. Patterson AJ, Garway-Heath DF, Strouthidis NG, Crabb DP. A new statistical approach for quantifying change in series of retinal and optic nerve head topography images. *Invest Ophthalmol Vis Sci* 2005;46(5):1659–1667. [PubMed: 15851566]
3. Balasubramanian M, Zabic S, Bowd C, et al. A framework for detecting glaucomatous progression in the optic nerve head of an eye using proper orthogonal decomposition. *IEEE Trans Inf Technol Biomed* 2009;13(5):781–793. [PubMed: 19369163]
4. Bowd C, Balasubramanian M, Weinreb RN, et al. Performance of confocal scanning laser tomograph topographic change analysis (TCA) for assessing glaucomatous progression. *Invest Ophthalmol Vis Sci* 2009;50(2):691–701. [PubMed: 18836168]
5. Sweldens W. The lifting scheme: a construction of second generation wavelets. *Siam J Math Anal* 1998;29(2):511–546.
6. Weinreb RN, Lusk M, Bartsch DU, Morsman D. Effect of repetitive imaging on topographic measurements of the optic nerve head. *Arch Ophthalmol* 1993;111(5):636–638. [PubMed: 8489444]
7. Burgoyne, CF.; Thompson, HW.; Mercante, DE.; Amin, R. Basic issues in the sensitive and specific detection of optic nerve head surface change within longitudinal LDT TopSS images: introduction to the LSU Experimental Glaucoma (LEG) study. In: Lemij, HG.; Schuman, JS., editors. *The Shape of Glaucoma*. The Hague, The Netherlands: Kugler Publications; 2000. p. 1-37.
8. Wang LW, Zhang Y, Feng JF. On the Euclidean distance of images. *IEEE Transactions on Pattern Analysis and Machine Intelligence* 2005;27(8):1334–1339. [PubMed: 16119271]
9. Artes PH, Chauhan BC. Longitudinal changes in the visual field and optic disc in glaucoma. *Prog Retin Eye Res* 2005;24(3):333–354. [PubMed: 15708832]
10. Chauhan BC, McCormick TA, Nicoleta MT, LeBlanc RP. Optic disc and visual field changes in a prospective longitudinal study of patients with glaucoma: comparison of scanning laser tomography with conventional perimetry and optic disc photography. *Arch Ophthalmol* 2001;119(10):1492–1499. [PubMed: 11594950]

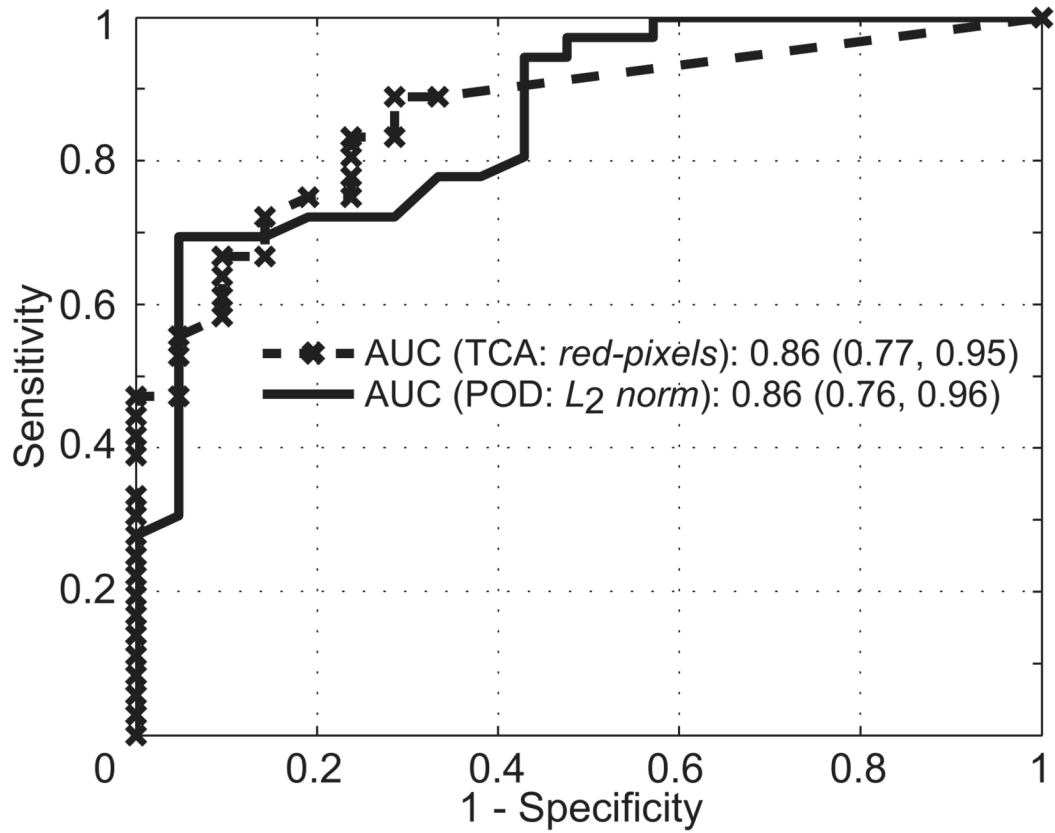


Figure 1. Comparative ROC curves of the POD L_2 norm and TCA total red pixels parameters in differentiating progressors from normal subjects. There was no difference in the AUC between the POD and TCA parameters.

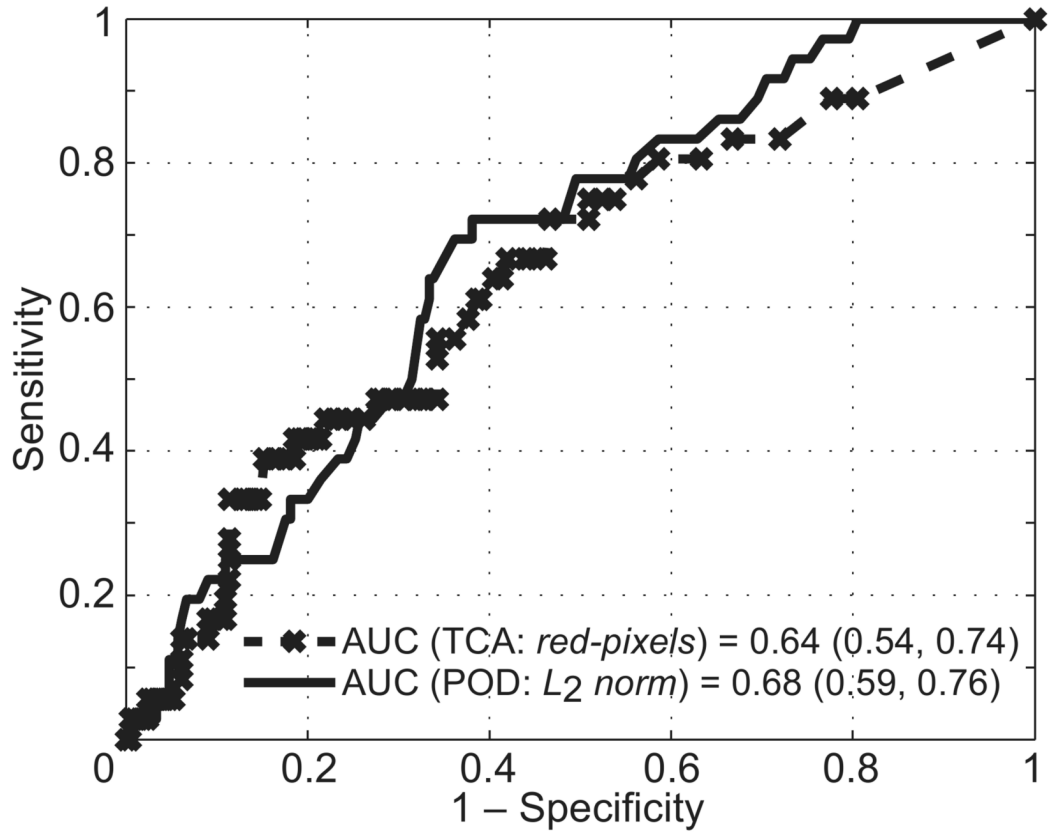


Figure 2. Comparative ROC curves of the POD L_2 norm and TCA total red pixels parameters in differentiating progressors from nonprogressors. The difference in their AUCs of 0.04 (95% CI = -0.08-0.14; $P = 0.28$) was not statistically significant.

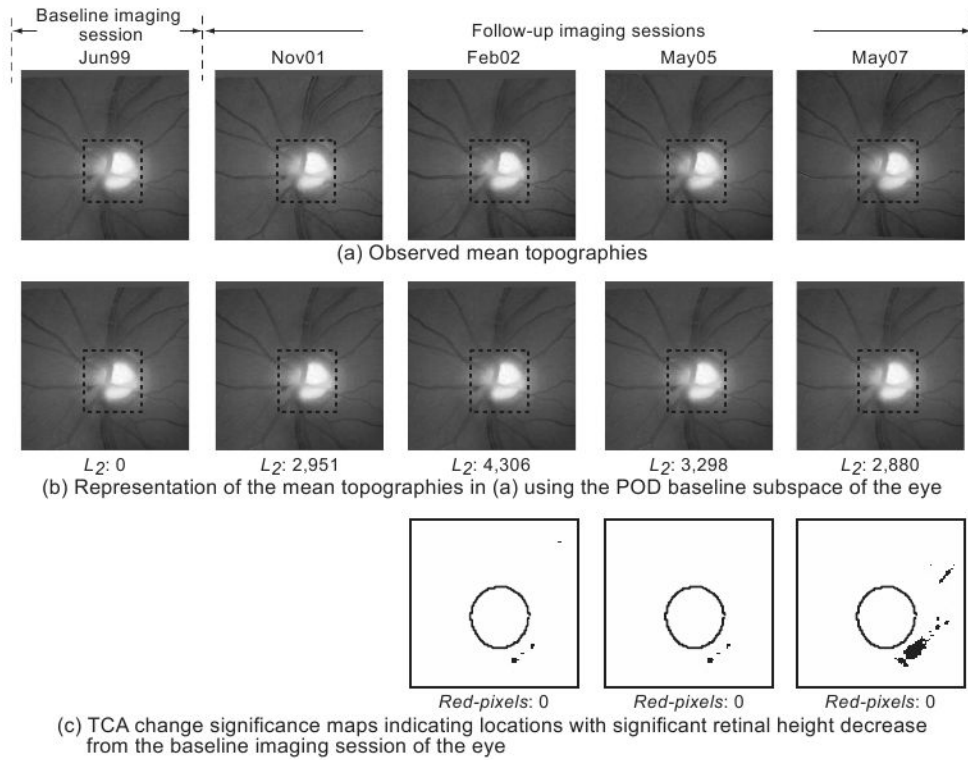


Figure 3. HRT-II follow-up examinations of a normal subject. In the POD framework, summary parameters were calculated by comparing the topographic measurements within the optic disc region (marked by *dotted rectangles* in **a** and **b**) in the observed follow-up topographies (**a**) with their respective baseline subspace representations (**b**). It can be visually observed that the follow-up topographies in (**a**) appear more similar to their baseline subspace representations in (**b**) indicating less change from baseline. Quantitatively, the L_2 norm of 2,880 in the last follow-up of the normal subject in (**b**) is lower (indicating less change) than the L_2 norm of 20,974 in the last follow-up of the progressor shown in Fig. 4b). For TCA, the red pixel count within the optic disc margin (**c**) was used to identify the degree of change from baseline.

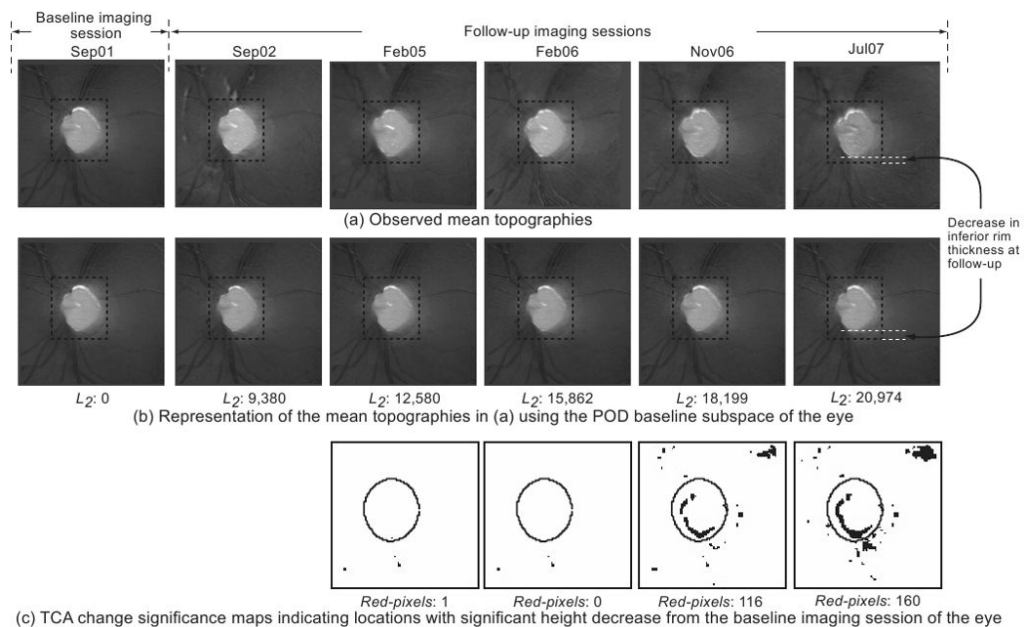


Figure 4.

HRT-II follow-up topographies of a progressor. In the POD framework, rim thinning can be observed in the inferior optic disc location (between the 5 and 8 o'clock positions) in (b) by visually comparing the observed follow-up topographies in (a) with their respective baseline subspace representations shown immediately below them in (b). Rim thinning may not be visually obvious in the follow-up topographies in (a) because retinal topographic measurements have a wider range; therefore, for demonstration, inferior rim thickness at baseline and the follow-up on Jul07 are manually marked in (a) and (b). In addition, enlarged topographies, reflectance images, stereophotographs, and visual function GPA from Jul07 are shown in Figure 5 for a closer visual inspection. Quantitatively, the L_2 norm of 20,974 in the last follow-up of the progressor in (b) is higher (indicating more change) compared with the L_2 norm of 2,880 in the last follow-up of the normal shown in Figure 3b. TCA detected superpixel locations with significant decrease in retinal height, shown as black pixels in (c).

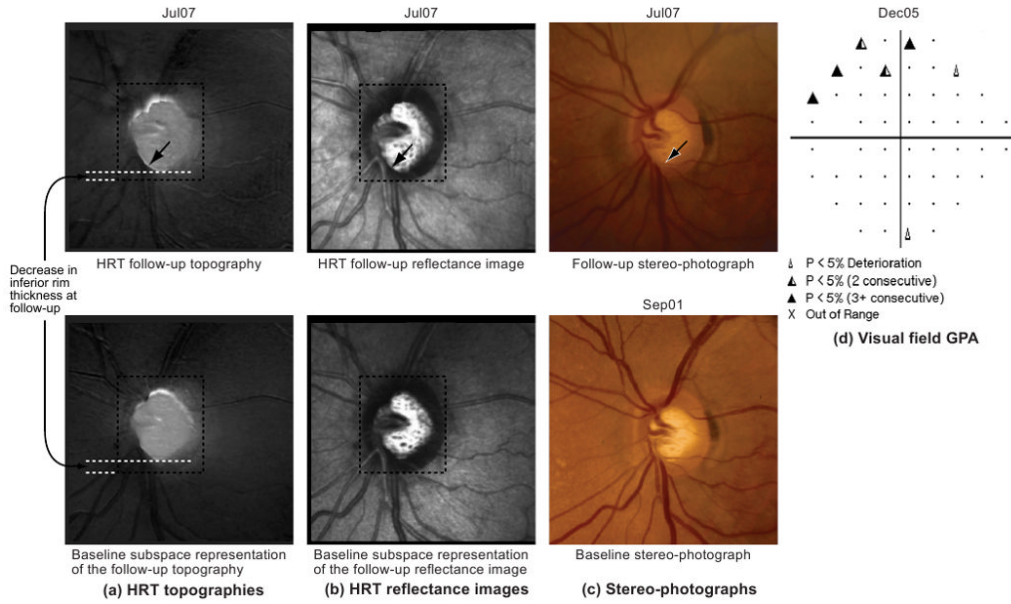
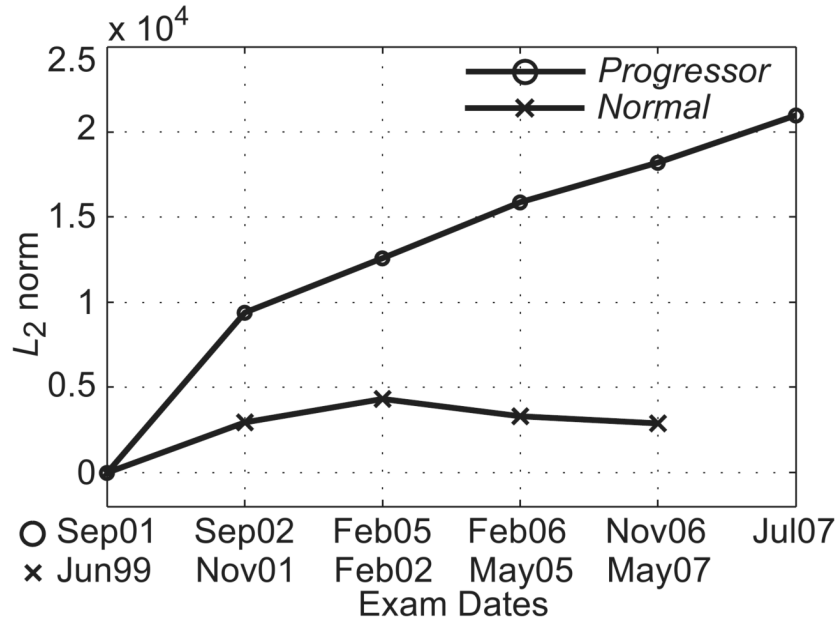
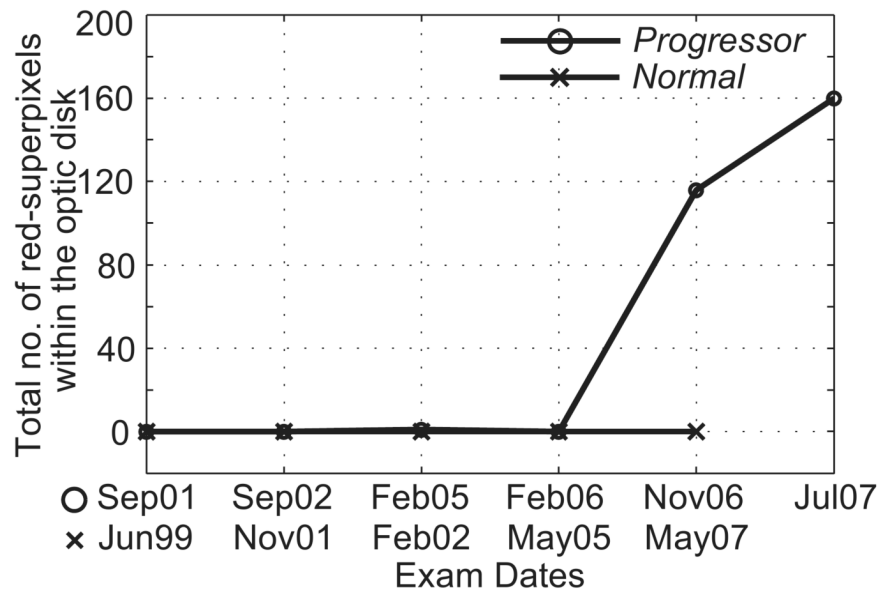


Figure 5. (a) HRT topographies of the last follow-up examination; (b) HRT reflectance images of the last follow-up examination; (c) stereophotographs of the baseline and last follow-up examinations, and (d) SAP visual field GPA of the example progressor shown in Figure 4. Neuroretinal rim thinning and an eventual enlargement of the optic cup can be observed in the inferior optic disc, between 5- and 8-o'clock, in (a–c, arrow). Corresponding visual field changes can be observed in the superior hemifield location (d). Topographic changes may not be visually obvious in (a) because retinal topographic measurements have a wider range; therefore, for demonstration, inferior rim thickness at baseline and follow-up are marked in the topographies in (a).

(a) POD L_2 norm parameter trends

(b) TCA red-pixels parameter trends

Figure 6.

(a) POD L_2 norm trends and (b) TCA red pixel parameter trends of a normal (Fig. 3) and a progressor (Fig. 4) eye.

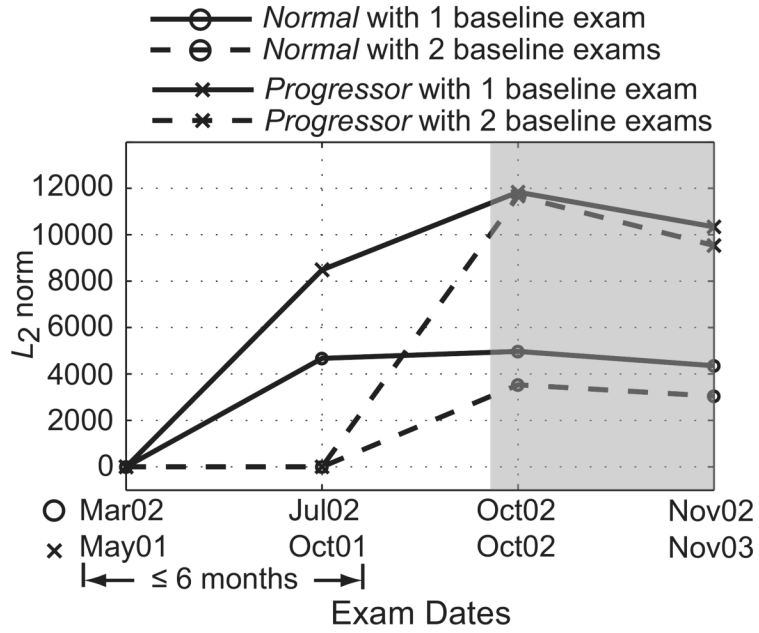


Figure 7. POD L_2 norm parameter trend plot of an example progressor and a normal eye indicate the ability of the POD framework to improve the variability estimates at baseline when using two baseline examinations (i.e., the examinations from Mar02 and Jul02 for the normal eye and the examinations from May01 and Oct01 for the progressor). The shaded region in the plot highlights differences in the POD L_2 norm parameter, with one and two baseline examinations. The lower L_2 norms from the follow-up examinations of the normal eye (Oct02 and Nov02) when two baseline examinations were used compared with when one was used indicates that some of the differences observed in the follow-ups when using one baseline examination were due to nonglaucomatous measurement variations.

Table 1

A Summary of the Progressors and Nonprogressors Used for Evaluating the Performance of the POD Framework and TCA

	Nonprogressors	Progressors
Eyes (subjects), <i>n</i>	210 (148)	36 (33)
Age, y		
Mean (95% CI)	66.24 (64.24–68.24)	70.37 (67.26–73.48)
Median (range)	69.37 (22.74–88.97)	70.33 (52.44–90.23)
HRT exams, <i>n</i> , median (range)	4 (4–8)	5 (4–8)
HRT follow-up, y, median (range)	3.59 (1.65–7.40)	4.13 (2.38–6.96)
SAP mean deviation at baseline		
Mean (95% CI)	–1.72 (–2.16––1.28)	–3.65 (–5.45––1.84)
Median (range)	–0.95 (–30.13–2.20)	–2.15 (–21.74–1.72)
SAP PSD at baseline		
Mean (95% CI)	2.47 (2.18–2.76)	4.19 (2.87–5.51)
Median (range)	1.73 (0.85–13.32)	2.30 (0.99–13.18)
Abnormal disk [†] from photo evaluation at Baseline, %	45.24 (95/210 eyes)	77.14 (27/35 eyes)*
Abnormal visual field [‡] at baseline, %	32.86 (69/210 eyes)	52.78 (19/36 eyes)
Both abnormal disk [†] from photo evaluation and abnormal visual field [‡] at baseline, %	19.52 (41/210 eyes)	42.86 (15/35 eyes)*

* One of the eyes that progressed by SAP GPA of the 36 progressors did not have a baseline stereophotograph within 6 months of the HRT-II baseline date.

[†] Optic disc with cup-to-disk area, neuroretinal rim thinning, or retinal nerve fiber defects indicative of glaucoma.

[‡] Visual field PSD with $P \leq 0.05$ and/or Glaucoma Hemifield Test results outside normal limits by STATPAC analysis.

Table 2
Diagnostic Accuracy of the POD Framework and TCA for 36 Progressors, 21 Normal Subjects, and 210 Nonprogressors*

	TCA			POD Framework		
	Red Pixels [†]	CSIZE [‡]	CSIZE % of Disc Size	L ₂ Norm	IMED	Correlation
AUC (95% CI)						
Progressors vs. normal subjects	0.86 (0.77–0.95)	0.86 (0.77–0.95)	0.86 (0.77–0.95)	0.86 (0.76–0.96)	0.85 (0.75–0.95)	0.70 (0.56–0.84)
Progressors vs. nonprogressors	0.64 (0.54–0.74)	0.63 (0.53–0.73)	0.63 (0.53–0.73)	0.68 (0.59–0.76)	0.67 (0.59–0.76)	0.63 (0.53–0.72)

* Respective parameters from the last HRT-II examinations of the study eyes were used for ROC analysis.

[†] Total number of significant superpixel change locations inside the optic disk margin, in superpixels.

[‡] Size of the largest cluster of superpixel change locations inside the optic disk margin, in superpixels.